

MSSM Higgs particles in the intense-coupling regime*

MARGARETE M. MÜHLLEITNER[†]

Laboratoire de Physique Mathématique et Théorique, UMR5825-CNRS,
Université de Montpellier II, F-34095 Montpellier Cedex 5, France.

Abstract

In the “intense-coupling” regime all Higgs bosons of the Minimal Supersymmetric extension of the Standard Model (MSSM) are rather light and have comparable masses of $\mathcal{O}(100 \text{ GeV})$. They couple maximally to electroweak gauge bosons, and for large ratios of the vacuum expectation values of the two Higgs doublet fields, $\tan \beta$, they interact strongly with the standard third generation fermions. We present in this note a comprehensive study of this scenario. We summarize the main phenomenological features, and the accordance with the direct constraints from Higgs boson searches at LEP2 and the Tevatron as well as the indirect constraints from precision measurements will be checked. After the presentation of the decay branching ratios, we discuss the production cross sections of the neutral Higgs particles in this regime at future colliders, the Tevatron Run II, the LHC and a 500 GeV e^+e^- linear collider.

*To appear in the proceedings of the 10th International Conference on Supersymmetry and Unification of Fundamental Interactions (SUSY02), June 17-23, 2002, DESY Hamburg. Talk based on the collaboration with E. Boos, A. Djouadi and A. Vologdin [1].

[†]Present address: Paul Scherrer Institut, CH-5232 Villigen PSI, Switzerland; email: Margarete.Muehleitner@psi.ch

1 Introduction

The Higgs sector of the MSSM consists of five physical Higgs states, two CP-even Higgs bosons, h and H , a CP-odd A and two charged H^\pm bosons [2]. Supersymmetric relations imply that at least the lightest one, h , has a mass below ~ 130 GeV after including radiative corrections [3] and will therefore be accessible at future pp and e^+e^- colliders. In the decoupling regime [4], the H , A and H^\pm bosons are very heavy and degenerate, and the light h state behaves Standard Model (SM) like. Being of $\mathcal{O}(1 \text{ TeV})$ the heavy Higgs particles might escape detection so that the MSSM cannot be disentangled from the SM. A much more interesting scenario would be the opposite non-decoupling regime where all Higgs bosons are rather light and have comparable masses. In the case of large values of $\tan\beta$ one of the CP-even bosons will be almost degenerate in mass with A and have almost the same couplings as the pseudoscalar Higgs boson, while the other CP-even Higgs boson behaves SM-like. In this situation all Higgs bosons will be accessible at the next generation of colliders in a plethora of production and decay processes with rates that can be very different from the SM case. Since the Higgs bosons are almost degenerate, several production channels have to be considered at the same time in order to detect the particles individually.

In the following, we discuss this intense-coupling regime taking into account direct and indirect experimental constraints. The various decay branching ratios will be presented, and the production at future colliders, the Tevatron Run II [5, 6], the LHC [6, 7] and e^+e^- machines [8], will be analyzed.

2 The MSSM Higgs sector in the intense-coupling regime

The properties of the MSSM Higgs bosons are defined by their four masses, the ratio $\tan\beta$ and the mixing angle α , introduced to diagonalize the Higgs boson mass matrix in the CP-even sector. Due to supersymmetry (SUSY), at tree level there are only two independent parameters, in general taken to be the A boson mass, M_A , and $\tan\beta$. Radiative corrections introduce a further dependence on other soft SUSY breaking parameters [3]. The intense-coupling regime is characterized by rather light, almost degenerate Higgs bosons and large values of $\tan\beta$. Taking into account the leading radiative corrections in the case of large $\tan\beta$ for the Higgs boson masses and the couplings to fermions and gauge bosons, rather simple and accurate formulae can be derived, from which the features of the Higgs boson sector in this non-decoupling scenario can be read off [1]: The Higgs states are almost degenerate in mass, with

$$\begin{aligned} 90 &\lesssim M_\Phi \lesssim 130 \text{ GeV}, & \Phi = h, H, A \\ M_{H^\pm} &\lesssim 150 \text{ GeV} \end{aligned} \tag{1}$$

For large values of $\tan\beta$ one of the CP-even Higgs bosons, denoted by Φ_A in the following, is degenerate in mass with A and has large couplings to b quarks and τ leptons, *i.e.* it behaves like a A boson, whereas the other CP-even Higgs boson, denoted by Φ_H , behaves SM-like with maximal couplings to gauge bosons and strong couplings to top quarks. Depending on whether the A boson mass value is below or above a critical mass value M_C , the respective role is taken over by h or H :

$$M_A \geq M_C : M_H = M_A \quad \text{and} \quad H = \Phi_A \qquad M_h = M_C \quad \text{and} \quad h = \Phi_H$$

$$M_A \leq M_C : M_h = M_A \quad \text{and} \quad h = \Phi_A \quad M_H = M_C \quad \text{and} \quad H = \Phi_H \quad (2)$$

The critical mass M_C is approximatively given by

$$M_C = \sqrt{M_Z^2 + \epsilon} \quad \text{with} \quad (3)$$

$$\epsilon = \frac{3G_F}{\sqrt{2}\pi^2} \left\{ \frac{\overline{m}_t^4}{\sin^2 \beta} \left[t + \frac{X_t}{2} \right] - \left[\frac{\overline{m}_t^2 M_Z^2 t}{2} + \frac{2\alpha_s}{\pi} \frac{\overline{m}_t^4}{\sin^2 \beta} (X_t t + t^2) \right] \right\} \quad (4)$$

where

$$t = \log \frac{M_S^2}{m_t^2} \quad \text{and} \quad X_t = \frac{2A_t^2}{M_S^2} \left(1 - \frac{A_t^2}{12M_S^2} \right) \quad (5)$$

G_F denotes the Fermi constant, \overline{m}_t the running $\overline{\text{MS}}$ top quark mass at the scale $M_t = 175$ GeV, to account for the leading QCD corrections, α_s the strong coupling constant at M_t , A_t the stop trilinear coupling and M_S the common SUSY breaking mass scale. For $M_A \gg M_C$, the decoupling limit is reached and h behaves SM-like, cf. (2).

3 Experimental constraints on the intense-coupling regime

3.1 Direct constraints

The search for Higgs bosons at LEP2 in the Higgs-strahlung process, $e^+e^- \rightarrow ZH^0$, has set a lower bound on the SM Higgs boson mass, $M_{H^0} > 114.4$ GeV at the 95% confidence level [9]. In the MSSM, this bound is valid for the lighter CP-even Higgs boson h if its coupling to Z bosons is SM-like, $g_{ZZh}^2/g_{ZZH^0}^2 \equiv \sin^2(\beta - \alpha) \approx 1$, or for the heavier CP-even state H in the case of a SM-like ZZH coupling, $g_{ZZH}^2/g_{ZZH^0}^2 \equiv \cos^2(\beta - \alpha) \approx 1$. In addition, the search for Higgs bosons in the associated production process $e^+e^- \rightarrow Ah$ sets the limits $M_h > 91.0$ GeV and $M_A > 91.9$ GeV at the 95% confidence level [9]. In order to derive a bound on M_h for arbitrary values of M_A and $\tan \beta$ we have fitted the exclusion plots for $\sin^2(\beta - \alpha)$ and $\cos^2(\beta - \alpha)$ versus M_h and $M_A + M_h$, respectively, given in [9], and delineated the regions allowed by the LEP2 data up to $\sqrt{s} = 209$ GeV in the $[M_A, \tan \beta]$ and $[M_h, \tan \beta]$ planes [1]. Fig. 1 shows the domains allowed by the LEP2 constraints for the no-mixing scenario, *i.e.* the trilinear soft SUSY breaking coupling in the stop sector $A_t = 0$ TeV, and the maximal mixing scenario, $A_t \approx \sqrt{6}$ TeV. In the maximal mixing scenario, the allowed region is larger, since the large stop mixing increases the maximal M_h value to the level where it exceeds the discovery limit, $M_h \gtrsim 114$ GeV.

The red and the green regions show the implication of the 2.1σ evidence for a SM-like Higgs boson with a mass $M_{\Phi_H} = 115.6$ GeV [9]. Considering the theoretical and experimental uncertainties, this result has been interpreted as favoring the mass range $114 \text{ GeV} \lesssim M_{\Phi_H} \lesssim 117 \text{ GeV}$. Since this Higgs boson should be SM-like, the additional constraint $g_{ZZ\Phi_H}^2/g_{ZZH^0}^2 \geq 0.9$ has been imposed. As can be seen in Fig. 1, the H boson can be the “observed” Higgs boson only in the case of zero mixing. For large stop mixing, the H boson mass always exceeds 117 GeV.

Fig. 1 demonstrates that the intense-coupling regime, where $90 \text{ GeV} \lesssim M_\Phi \lesssim 130 \text{ GeV}$ [$\Phi = h, H, A$] and $\tan \beta \gg 1$, is still allowed by the LEP2 searches.

Further constraints can be obtained from the Higgs boson searches at the Tevatron [6]. The search for the top decay mode into a b -quark and a charged Higgs boson, $t \rightarrow bH^+$,

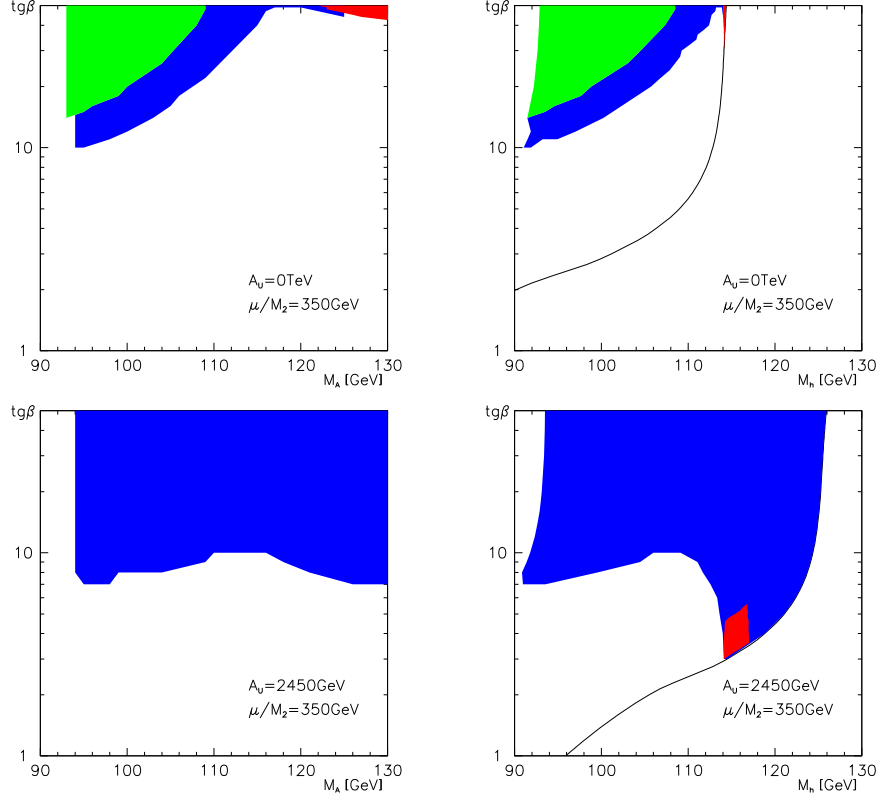


Figure 1: The allowed regions for M_A [left] and M_h [right] from LEP2 searches as a function of $\tan\beta$ (colored regions) in the case of no mixing (up) and maximal mixing (down). The red regions indicate where $114 \text{ GeV} < M_h < 117 \text{ GeV}$ and $g_{ZZh}^2/g_{ZZH^0}^2 > 0.9$, and the green regions indicate where $114 \text{ GeV} < M_H < 117 \text{ GeV}$ and $g_{ZZH}^2/g_{ZZH^0}^2 > 0.9$.

sets the limits $\tan\beta \lesssim 50$ for $M_{H^\pm} \lesssim 150 \text{ GeV}$ (i.e. $M_A \lesssim 130 \text{ GeV}$). The data on $\tau^+\tau^- + 2$ jets can be exploited to derive limits from the process $pp \rightarrow b\bar{b}A$, leading to $\tan\beta \lesssim 80$ for $M_A \lesssim 130 \text{ GeV}$. In summary, the intense-coupling regime is not excluded by the Tevatron data.

3.2 Indirect constraints

Indirect constraints on the parameters of the MSSM Higgs sector come from high precision data [10]. We examined the contributions of the MSSM Higgs sector in the intense-coupling regime [1] and found that they do not violate the experimental constraints on the ρ parameter (the new physics contribution is limited to $\Delta_\rho^{NP} \lesssim 1.1 \cdot 10^{-3}$), the anomalous magnetic moment ($a_\mu = 11659202(20) \cdot 10^{-10}$), the $Zb\bar{b}$ vertex (the forward-backward asymmetry of the decay $Z \rightarrow b\bar{b}$ is $A_{FB}^b = 0.099 \pm 0.002$) and the $b \rightarrow s\gamma$ decay (the branching ratio is given by $BR(b \rightarrow s\gamma) = (3.37 \pm 0.37 \pm 0.34 \pm 0.24_{-0.16}^{+0.35} \pm 0.38) \cdot 10^{-4}$).

4 Branching ratios and total widths

Fig. 2 shows the branching ratios of the neutral Higgs bosons A, h, H as a function of their respective mass for $90 \lesssim M_A \lesssim 130 \text{ GeV}$ and $\tan\beta = 30$. As can be inferred from the figure, the A boson decays with a ratio of 90% into $b\bar{b}$ and of 10% into $\tau^+\tau^-$, the other branching ratios being below $\sim 10^{-3}$. The pattern for the branching ratios of the

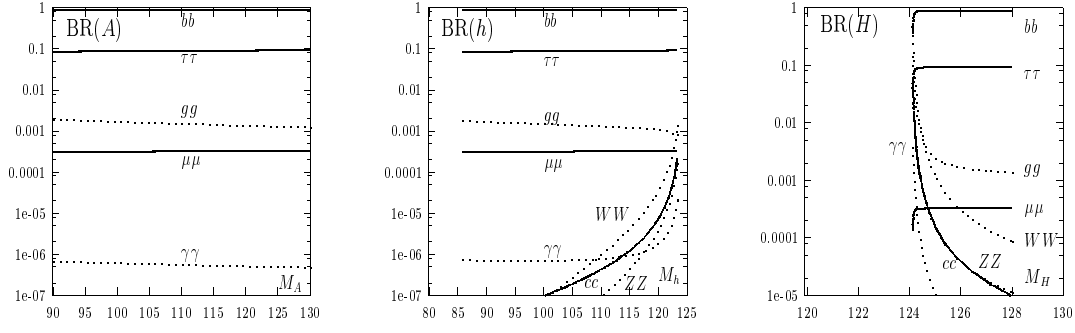


Figure 2: *The branching ratios of the neutral Higgs bosons A (left), h (middle), H (right) as a function of their masses for $\tan\beta = 30$ and $\mu = M_2 = 1$ TeV, $M_S = 1$ TeV, $A_t = 2.6$ TeV.*

CP-even Higgs bosons is similar to that of the A boson if their masses are close to M_A and $\tan\beta \gg 1$, unless h and H have masses close to M_C , where they behave SM-like. In practice, however, this limit is not reached, especially for h with $\tan\beta \lesssim 50$. As can be seen in Fig. 2, the h branching ratios are all below $\sim 10^{-3}$ except for the $b\bar{b}$ and $\tau^+\tau^-$ final states. This is because the h coupling to gauge bosons does not reach the SM limit, while the $hb\bar{b}$ coupling is still enhanced for large $\tan\beta$. In the case of H and $M_H \gtrsim 125$ GeV the branching ratios into $\gamma\gamma$, WW and gg are much smaller than in the SM. They approach the SM values near the critical mass. For larger values of $\tan\beta$, however, a new feature occurs. The H coupling to down type fermions becomes strongly suppressed and at some stage nearly vanishes, so that the branching ratios into WW , gg and $\gamma\gamma$ become larger than in the SM case in this pathological region [11], cf. Fig. 3.

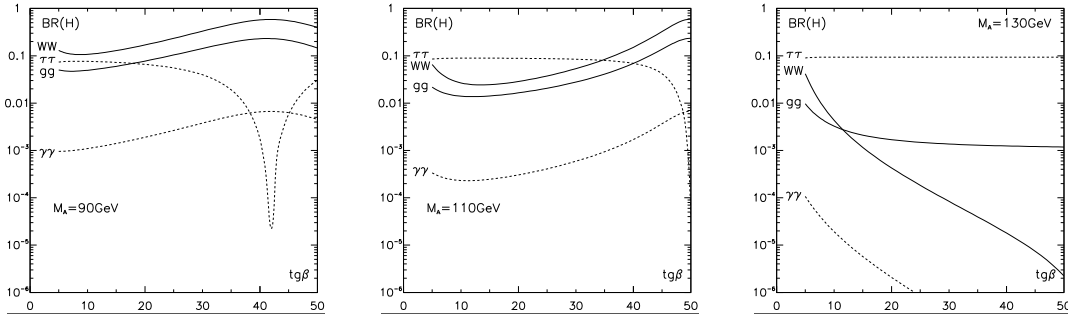


Figure 3: *The branching ratios of the H boson into $\gamma\gamma$, gg , W^+W^- , $\tau^+\tau^-$ final states as a function of $\tan\beta$ for $M_A = 90, 110, 130$ GeV.*

Finally, the total decay widths of h, H are SM-like for masses near M_C and therefore rather small. Otherwise, the total width of the Φ_A -like boson, dominated by the decays in b and τ , being proportional to $\tan^2\beta$, can become rather large for large $\tan\beta$ values [e.g. $\Gamma_{tot}^H \approx 7$ GeV for $\tan\beta = 50$, $M_A = 130$ GeV], cf. Fig. 4.

5 Production at Future Colliders

5.1 Production at pp colliders.

The neutral MSSM Higgs bosons can be produced in a plethora of processes at Tevatron

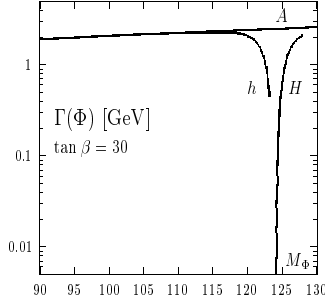


Figure 4: The total decay widths of the neutral Higgs bosons h, H, A as a function of their masses for $\tan \beta = 30$.

Run II and the LHC. Fig. 5 shows the main production processes at the LHC for $\tan \beta = 30$, *i.e.* gluon-gluon fusion, $gg \rightarrow \Phi$ [$\Phi = h, H, A$], associated production, $gg, q\bar{q} \rightarrow \Phi + b\bar{b}/t\bar{t}$, and WW/ZZ fusion, $VV \rightarrow h, H$ [$V = W, Z$]. For large $\tan \beta$ the gg fusion process is dominated by the b quark loop contributions, which are enhanced by $\tan^2 \beta$ factors, leading to cross sections of up to 1500 pb for the Φ_A -like bosons. Due to the large QCD backgrounds, only the $\gamma\gamma$ final states can be probed. In the intense-coupling

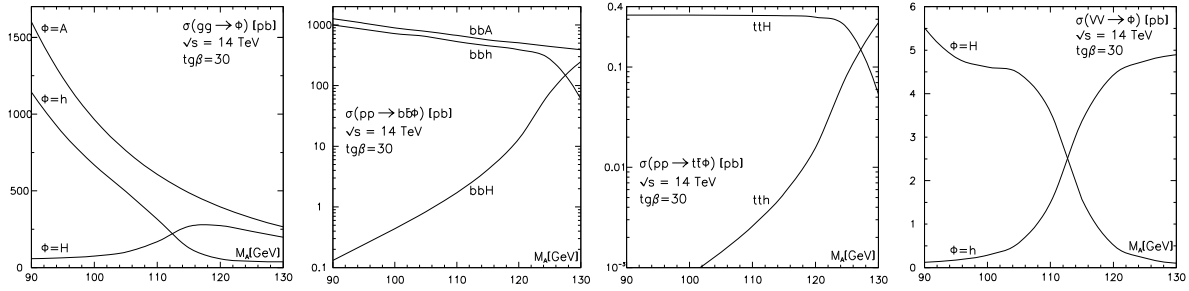


Figure 5: Production processes at the LHC for the gluon-gluon fusion process, associated production with b quarks and with top quarks, and the WW/ZZ fusion processes (from left to right) as a function of M_A for $\tan \beta = 30$ with the same SUSY parameters as in Fig. 2. The next-to-leading order QCD corrections have been taken into account, where available [12].

regime there can be situations, however, where the rates $\sigma(gg \rightarrow \Phi) \times BR(\Phi \rightarrow \gamma\gamma)$ are small for all three Higgs bosons, due to small cross sections, cf. Fig. 5, or small branching ratios into $\gamma\gamma$ in the case, where the SM limit is not yet reached, cf. Fig. 2. The A, Φ_A production processes in association with b quarks are strongly enhanced by $\tan^2 \beta$ factors, reaching rates similar to the gg fusion process, whereas the $\Phi_H b\bar{b}$ cross section is much smaller due to a tiny Yukawa coupling. The detection of A and Φ_A , however, is promising, since the additional two b quarks in the final state can be exploited to reduce the QCD backgrounds and one does not have to rely on the decays into photons or massive gauge bosons. The associated production cross sections with t quark pairs are suppressed due to the smaller phase space and a not enhanced Higgs- $t\bar{t}$ coupling. To the contrary, the $A/\Phi_A t\bar{t}$ process is strongly suppressed by $\tan^2 \beta$ factors. Only the $\Phi_H t\bar{t}$ production reaches cross sections at the level of ~ 0.3 pb. For the detection, the $\gamma\gamma$ and the $b\bar{b}$ final states can be exploited. The latter being more promising due to slightly enhanced branching ratios compared to the SM case, cf. Fig. 2. The vector boson fusion processes are two to three orders of magnitude smaller than the $gg \rightarrow \Phi$ and $b\bar{b}\Phi$ processes, reaching ~ 5 pb

only for the SM-like Higgs boson with maximal coupling to the gauge bosons. In this case the $\tau^+\tau^-$ final states would allow for the detection by taking advantage of the energetic quark jets in the forward and backward directions [13]. The corresponding cross sections at the Tevatron show the same pattern being a factor 30 to 150 smaller depending on the process [1].

5.2 Production at e^+e^- colliders.

The main production processes at e^+e^- colliders [14] are the bremsstrahlung process, $e^+e^- \rightarrow Z + h, H$, the associated production process, $e^+e^- \rightarrow A + h, H$, the vector boson fusion, $e^+e^- \rightarrow \bar{\nu}_e\nu_e/e^+e^- + h, H$, and the radiation off top and b quarks, respectively, $e^+e^- \rightarrow t\bar{t}/b\bar{b} + \Phi$, cf. Fig. 6. Since the cross sections for Higgs-strahlung and Higgs pair production as well as the cross sections for the h and H production are mutually complementary to each other, and in view of the high luminosity that can be reached at an e^+e^- collider [8] as well as the efficient b -quark tagging, all neutral Higgs bosons can be discovered at e^+e^- machines in the intense-coupling regime. Furthermore, in the associated production processes with quark pairs, the $t\bar{t}\Phi_H$ and for large enough $\tan\beta$, the $b\bar{b}A$, $b\bar{b}\Phi_A$ Yukawa couplings can be measured.

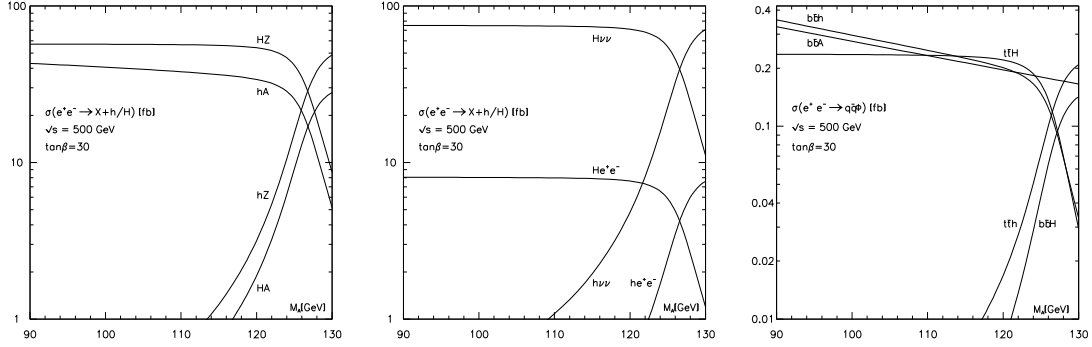


Figure 6: *Higgs production cross sections at a 500 GeV e^+e^- linear collider in the bremsstrahlung and associated Higgs production processes (left), the vector boson fusion processes (middle) and the associated production with top and bottom quarks (right) as a function of M_A for $\tan\beta = 30$. The SUSY parameters have been chosen as in Fig. 2.*

6 Summary

The preceding discussion has demonstrated that the phenomenology of the MSSM Higgs bosons in the intense-coupling regime is extremely rich. Being rather light, all Higgs bosons will be accessible at future colliders in various and complementary production channels. New features occurring in this scenario demand in some cases other techniques for the search of these particles than in the SM case and in the MSSM case close to the decoupling limit. Since the Higgs bosons are close in mass, it might be difficult to separate them, and several production channels have to be considered at the same time. In addition, the large total widths for the pseudoscalar and pseudoscalar-like Higgs boson lead to broader signals. Finally, the clean $\gamma\gamma$ final state signatures used for the Higgs boson searches at the LHC, might be much less frequent than in the SM case. Having summarized the main features of the intense-coupling regime in this note, more detailed Monte-Carlo studies are needed to assess at which extent these Higgs particles can be

discovered and their properties can be measured at future colliders.

Acknowledgments

I would like to thank my collaborators E. Boos, A. Djouadi and A. Vologdin for the fruitful collaboration on this project. This work has been supported by the European Union under contract HPRN-CT-2000-00149.

References

- [1] For details see: E. Boos, A. Djouadi, M. Mühlleitner and A. Vologdin, Phys. Rev. D66 (2002) 055004, [hep-ph/0205160].
- [2] For a review on the Higgs sector of the MSSM, see J.F. Gunion, H.E. Haber, G.L. Kane and S. Dawson, “The Higgs Hunter’s Guide”, Addison–Wesley, Reading 1990.
- [3] See *e.g.* M. Carena and H.E. Haber, hep-ph/0208209, and references therein.
- [4] See *e.g.* H. Haber, hep-ph/9505240 and more recently A. Dobado, M.J. Herrero and S. Penaranda, Eur. Phys. J. C17 (2000) 487.
- [5] S. Abel et al., Report of the SUGRA working group for RUN II of the Tevatron, hep-ph/0003154.
- [6] D. Cavalli et al., Higgs report for the Les Houches 2001 Workshop “Physics at TeV colliders”, hep-ph/0203056.
- [7] ATLAS Collaboration, Technical Design Report CERN-LHCC 99-14; CMS Collaboration, Technical Proposal, Report CERN-LHCC 94-38.
- [8] E. Accomando, Phys. Rept. 299 (1998) 1; TESLA, Technical Design Report, hep-ph/0106315 and hep-ex/0108012; American Linear Collider Working Group, hep-ex/0106056; ACFA Linear Collider Working Group, hep-ph/0109166.
- [9] The LEP Higgs working group, hep-ex/0107029 and hep-ex/0107030; DELPHI Coll. (P. Abreu et al.), Phys. Lett. B499 (2001) 23; OPAL Coll. (G. Abbiendi et al.), Phys. Lett. B499 (2001) 38.
- [10] Particle Data Group (D.E. Groom et al.), Eur. Phys. J. C15 (2000) 1; The LEP Coll.s, the LEP EWWG and the SLD Heavy Flavor and EWWG, hep-ex/0103048; H.N. Brown et al. (muon ($g - 2$) Collaboration), Phys. Rev. Lett. 86 (2001) 2227.
- [11] M. Carena, S. Mrenna and C.E.M. Wagner, Phys. Rev. D62 (2000) 055008.
- [12] M. Spira et al., Nucl. Phys. B453 (1995) 17; A. Djouadi and M. Spira, Phys. Rev. D62 (2000) 014004.
- [13] T. Plehn, D. Rainwater and D. Zeppenfeld, Phys. Rev. D61 (2000) 093005.
- [14] A. Djouadi, J. Kalinowski and P.M. Zerwas, Z. Phys. C54 (1992) 255 and Z. Phys. C57 (1993) 569.